Available online at www.sciencedirect.com

ScienceDirect

Ceramics International 40 (2014) 1723–1727

CERAMICS INTERNATIONAL

www.elsevier.com/locate/ceramint

Luminescence properties and energy transfer investigations of $Sr_3AlO_4F:Ce^{3+}$, Tb^{3+} phosphor

Jiayue Sun*, Guangchao Sun, Yining Sun

School of Science, Beijing Technology and Business University, Beijing 100048, China

Received 1 July 2013; received in revised form 13 July 2013; accepted 14 July 2013
Available online 23 July 2013

Abstract

Ce^{3+} and Tb^{3+} co-doped Sr_3AlO_4F phosphors were synthesized by the conventional high temperature solid-state method. X-ray diffraction (XRD) was used to characterize the phase structure. The luminescence spectra and decay lifetime curves of Ce^{3+} have been measured to prove energy transfer (ET) from Ce^{3+} to Tb^{3+}. Under the excitation of near-ultraviolet light, $Sr_3AlO_4F:Ce^{3+},Tb^{3+}$ phosphors exhibited blue emission corresponding to the f–d transition of Ce^{3+} ions and green emission bands corresponding to the f–f transition of Tb^{3+} ions, respectively. Effective energy transfer occurred from Ce^{3+} to Tb^{3+} in Sr_3AlO_4F host due to the observed spectra overlap between the emission spectrum of Ce^{3+} ion and the excitation spectrum of Tb^{3+} ion. The energy transfer efficiency from Ce^{3+} ion to Tb^{3+} ion was also calculated to be 51%. Furthermore, the energy transfer from Ce^{3+} to Tb^{3+} in Sr_3AlO_4F host was demonstrated to be resonant type via a dipole–dipole interaction mechanism. The present Ce^{3+} and Tb^{3+} co-doped Sr_3AlO_4F phosphor may have potential use in the technology of white light-emitting diodes.

Keywords: Optical materials; X-ray diffraction; Luminescence; Energy transition; Lanthanides

1. Introduction

The energy problem has been paid more and more attention over the next quarter of a century as one of most challenging scientific questions [1]. Recently, considerable research has been focused on white light-emitting diodes (w-LEDs) as the next generation solid-state light since w-LEDs have many favorable advantages in comparison with conventional incandescent and fluorescent lamp, such as high luminous efficiency, energy-saving, long lifetime, and so on [2,3]. The first commercial w-LED was generated by combing an InGaN-based blue diode and YAG:Ce^{3+} ($Y_3A_{l5}O_{12}:Ce^{3+}$) yellow phosphor materials [4]. However, this kind of w-LEDs encounters a low color-rendering index (CRI) on account of insufficient red emission. To solve these problems, the combination of an UV chip with red, green, and blue phosphors has been proposed. This technology has a higher CRI and high tolerance to the UV chip's color variation as the white color is obtained only by phosphors [5,6]. Therefore, the development on the novel multi-color emission phosphor becomes a host in the field of optical materials.

The ordered oxyfluoride Sr_3AlO_4F belongs to the tetragonal I4/mcm space group with unit cell parameters $a=b=6.7819$ Å and $c=11.3662$ Å. In this crystal, there are two types of layer components run perpendicular to the c axis and separated from each other [7]. One layer consists of isolated AlO_4 tetrahedra with Sr^{2+} as an insert, and another layer is Sr_2F layer. Due to the feature of ordered structure, Sr_3AlO_4F was considered to be a promising host compound for new optical materials [8,9]. Moreover, as a class of host materials, it has been argued that the compounds containing oxygen and fluorine anions may possess the advantages of oxide and fluoride. That is, the chemical stability, high absorption in vacuum ultraviolet region and withstand high-energy electron bombardment for oxide [10,11], and low phonon frequency for fluoride [12].

Lanthanide ions are very well suited to use as sensitizer for luminescent material, because they have a rich energy level structure that allows for efficient spectral conversion. Two of the candidates for the sensitizer are Eu^{2+} and Ce^{3+}, which

*Corresponding author. Tel./fax : +86 10 6898 5467.
E-mail address: jiayue_sun@126.com (J. Sun).

0272-8842/$ - see front matter © 2013 Elsevier Ltd and Techna Group S.r.l. All rights reserved.
http://dx.doi.org/10.1016/j.ceramint.2013.07.069

show broad and strong absorption in the desired spectral region due to 5d→4f. In addition, as we all know, the energy transfer from donor to acceptor plays an important role in luminescence. Owning to the allowed 4f→5d broadband transition, Ce^{3+} is an efficient sensitizing donor in many hosts and efficiently transfer the excitation energy to the $^5D_4$ state of Tb^{3+} [13]. Furthermore, for practical applications it would be important if Ce^{3+} could greatly enhance the emission of Tb^{3+}, because cheaper CeO_2 could be used partly to replace expensive Tb_4O_7. Therefore, Ce^{3+} and Tb^{3+} would be a good pair to act as a sensitizer and activator in the energy transfer from Ce^{3+} to Tb^{3+} in various hosts [14–19]. For instance, Guo et al discussed the Ce^{3+}–Tb^{3+} interaction by fluorescent method and calculated the possibility and efficiency of energy transfer from Ce^{3+} to Tb^{3+} in $Ba_2Gd_2Si_4O_{13}$. The analogical energy transfer was also studied by Luo et al in SrF_2 [20]. They demonstrated the possible energy transfer mechanism and quantitatively assessed this process, proving that the energy transfer from Ce^{3+} to Tb^{3+} can be illustrated by a dipole–dipole interaction mechanism with a critical distance of 1.6 nm.

In this Paper, the Ce^{3+}, Tb^{3+} and Ce^{3+}/Tb^{3+} co-doped Sr_3AlO_4F phosphors for w-LEDs were prepared by a solid-state reaction. We focus on the energy transfers from the near-ultraviolet light to visible light, which show high photoelectric conversion efficiency and a novel material of Ce^{3+}–Tb^{3+} co-doped Sr_3AlO_4F phosphors has been demonstrated, and the photoluminescence properties, decay time, especially the energy transfer process and mechanism of $Sr_3AlO_4F:Ce^{3+}$, Tb^{3+} phosphor were discussed in detail.

2. Experimental details

2.1. Preparation of $Sr_3AlO_4F:RE^{3+}$ phosphors

All the $Sr_3AlO_4F:RE^{3+}$ phosphors were prepared by a conventional solid-state reaction. The raw materials were a mixture of reagent grade SrF_2 (A.R.), $SrCO_3$ (A.R.), Al_2O_3 (A.R.), CeO_2 (99.999%) and Tb_4O_7 (99.999%). In general, the different valence states of rare earth ions and Sr^{2+} ion require a charge compensation mechanism. For this reason, the nonstoichiometry of this host lattice $Sr_{(6-3x)/2}RE_xAlO_4F$ was performed in actual experiment without adding the charge compensator ions (Li^+, Na^+). The composition for each material was weighted in proper stoichiometric ratio and mixed thoroughly in an agate mortar. The mixture samples were thoroughly mixed and heated for 4 h in the CO atmosphere at 1200 °C to insure the complete reduction of Ce and Tb.

2.2. Characterization

The X-ray diffraction (XRD) patterns were performed on a Shimadzu model XRD-6000 X-ray powder diffraction with Cu Kα radiation, 40 kV, 30 mA. The excitation and emission spectra were recorded by using a Hitachi F-7000 fluorescence spectrophotometer, and a 150 W Xe lamp was used as the excitation lamp. Luminescent decay curves were measured by using a FluoroLog-3 spectrofluorometer (HORIBA, USA) with a Nano-LED (N-250) as the excitation source and a R928P photomultiplier for signal detection. All the measurements were performed at room temperature.

3. Results and discussion

3.1. XRD analysis

Fig. 1 shows the XRD patterns of $Sr_3AlO_4F:RE^{3+}$. The diffraction peaks of all these samples can be exactly assigned to the pure tetragonal phase of Sr_3AlO_4F (space group: I4/mcm) according to JCPDS file (89-4485), indicating that the samples are single and pure phase, and RE^{3+} ions are completely incorporated into the host lattice by substituting for Sr^{2+} in the doping concentration range. The relative intensity of the diffraction peaks is slightly different from the standard card, which may relate to the preferential growth of the microcrystal particles under the given reaction condition. Since the ionic radii of Ce^{3+} (0.114 nm) or Tb^{3+} (0.104 nm) and Sr^{2+} (0.126 nm) are similar [21], Ce^{3+} and Tb^{3+} are expected to preferably occupy the Sr^{2+} site.

3.2. Luminescent properties of $Sr_3AlO_4F:Ce^{3+}$, Tb^{3+}

Fig. 2 illustrates the excitation and emission spectra of (a) Sr_3AlO_4F:1%Ce^{3+}, (b) Sr_3AlO_4F:1%Tb^{3+}, (c) Sr_3AlO_4F:1% Ce^{3+}, 1%Tb^{3+} phosphors. The excitation spectrum (Fig. 2(a)) monitored at 464 nm shows an intense band centered at 401 nm corresponding to 4f→5d transition of the Ce^{3+}. Moreover, under the 401 nm excitation, the emission spectrum displays an asymmetric broad band with a maximum around 464 nm, which is attributed to the 5d→4f transitions of Ce^{3+} [22]. Gaussian multi-peaks fit of the emission spectrum of Ce^{3+}-doped sample is shown in Fig. 3(a). It is clearly stated that the emission of Ce^{3+} can be divided into two peaks, one centered at 457 nm is due to the transition 5d→$^2F_{5/2}$, and the other peak centered at 493 nm is due to the transition 5d→$^2F_{7/2}$.

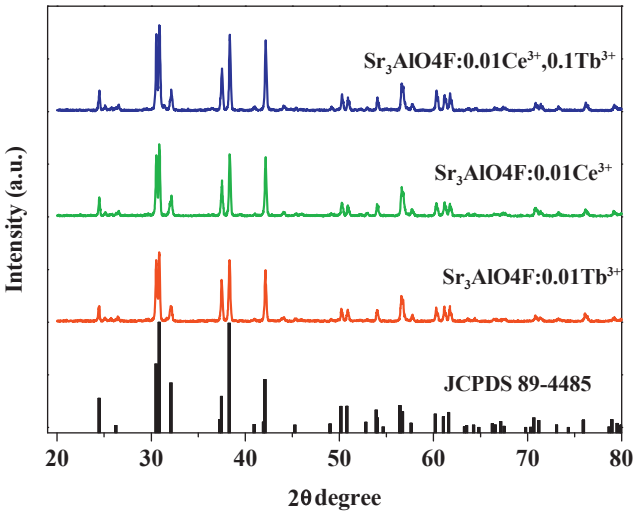

Fig. 1. XRD patterns of the $Sr_3AlO_4F:RE^{3+}$ (RE=Ce^{3+}, Tb^{3+}, Ce^{3+}/Tb^{3+}) as well as the standard data for Sr_3AlO_4F (JCPDS card no. 89-4485) used as a reference.

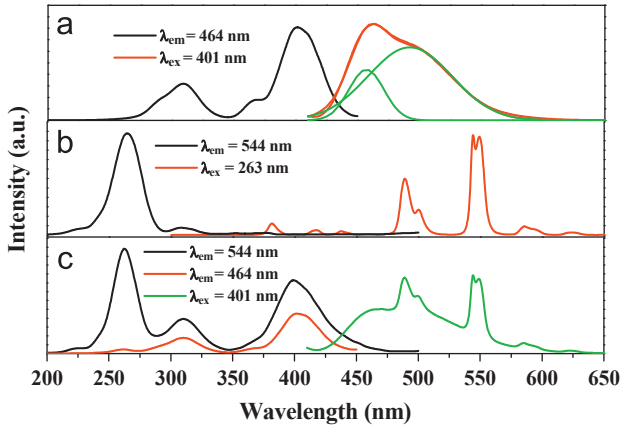

Fig. 2. The PLE and PL spectra of the single-doped and co-doped samples: (a) Sr_3AlO_4F:1%Ce^{3+}, (b) Sr_3AlO_4F:1%Tb^{3+}, (c) Sr_3AlO_4F:1%Ce^{3+}, 1%Tb^{3+}.

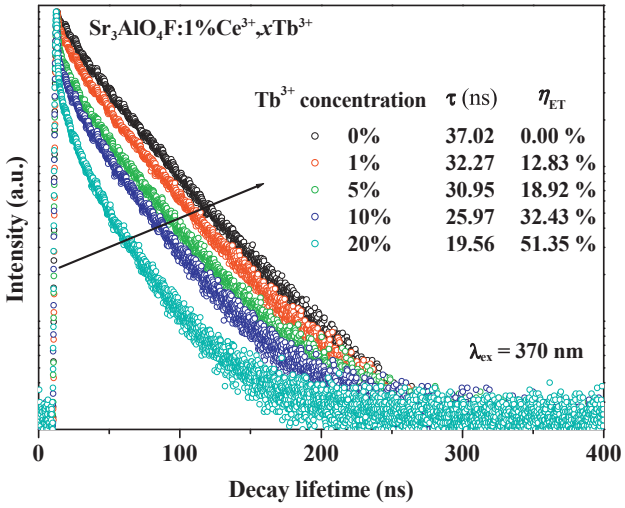

Fig. 3. Decay lifetimes of the Ce^{3+}:5d→4f luminescence of Sr_3AlO_4F: 1%Ce^{3+}, xTb^{3+} under excitation of 370 nm. Inset shows the decay lifetime and η_T of as a function of the Tb^{3+} concentration.

The two emission bands at 457 and 493 nm have an energy difference of about 1503 cm^{-1}, which is well agreement with the theoretical difference between the $^2F_{5/2}$ and $^2F_{7/2}$ levels of Ce^{3+} (~2000 cm^{-1}) [23].

The excitation and emission spectra of Sr_3AlO_4F: 1%Tb^{3+} are shown in Fig. 3(b). The excitation spectrum monitored at 544 nm consists of a strong band at 263 nm and a weak band at 308 nm, which correspond to the spin-allowed ($\Delta S=1$) and spin-forbidden ($\Delta S=0$) components of the $4f^8 \rightarrow 4f^7 5d^1$ transition [24]. The energy difference between these two transitions is 5411 cm^{-1}, agreeing well with the theoretical value (6000 cm^{-1}) reported previously [25–27]. Meanwhile, the Tb^{3+}-doped powder depicts a strong green emission excited by 263 nm. As indicated in the emission spectrum, four typical Tb^{3+} ions emission peaks centered at 623, 585, 544 and 489 nm are assigned to the transitions of $^5D_4 \rightarrow {}^7F_J$ (J=3, 4, 5, 6), and three weak bands centered at 437, 417 and 381 nm, which are ascribed to the transitions of $^5D_3 \rightarrow {}^7F_J$ (J=3, 4, 5). The dominated emission peak is at 544 nm. Fig. 2(a) and (b) clearly shows that there is a remarkable overlapping between emission band of Ce^{3+} (donor) and absorption band of Tb^{3+} (acceptor) in Sr_3AlO_4F, which declares that the possibility of energy transfer (ET) can occur from Ce^{3+} to Tb^{3+}.

Fig. 2(c) shows the PLE and PL spectra of Sr_3AlO_4F:1%Ce^{3+}, 1%Tb^{3+} sample. The excitation spectrum, monitored with the 544 nm emission ($^5D_4 \rightarrow {}^7F_5$) of Tb^{3+}, is composed of a strong band at 264 nm, a weak band at 308 nm, and an intense band at 401 nm. In comparison with the excitation spectra of Sr_3AlO_4F:1% Ce^{3+} (Fig. 2(a)) and Sr_3AlO_4F: 1%Tb^{3+} (Fig. 2(b)), the first band is ascribed to the $4f^8 \rightarrow 4f^7 5d^1$ transitions of Tb^{3+}, and the latter two bands originate from the 4f→5d transitions of Ce^{3+}, which indicates that energy transfer has occurred from Ce^{3+} to Tb^{3+} in the Sr_3AlO_4F:1%Ce^{3+}, 1%Tb^{3+} sample. Excitation into the Ce^{3+} excitation band at 401 nm yields both the emission of Ce^{3+} and that of Tb^{3+} ($^5D_4 \rightarrow {}^7F_J$ at 489, 544, 585, 623 nm), which is further indicative of the energy transfer from Ce^{3+} to Tb^{3+} in Sr_3AlO_4F host. Both the excitation and emission spectra in Fig. 2 imply an efficient energy transfer from Ce^{3+} to Tb^{3+} in Sr_3AlO_4F:1%Ce^{3+}, 1%Tb^{3+} sample.

3.3. Energy transfer from Ce^{3+} to Tb^{3+} in Sr_3AlO_4F:Ce^{3+}, Tb^{3+} phosphors

In Fig. 3, the decay curves for the Ce^{3+} 5d→4f emission at 464 nm are plotted with different Tb^{3+} concentration. It clearly illustrates that the lifetime of Ce^{3+} becomes shorter in the presence of a Tb^{3+} ion. The decay curves of Ce^{3+} ions can be well fitted to a double-exponential function [28]

$$I = A_1 \exp(-t/\tau_1) + A_2 \exp(-t/\tau_2) \quad (1)$$

where I is the luminescence intensity; A_1 and A_2 are constants; t is the time, and τ_1 and τ_2 are decay time for exponential components. The average luminescence lifetime for Ce^{3+} ions as a function of different Tb^{3+} concentration can be calculated by the formula

$$\tau = \frac{A_1\tau_1^2 + A_2\tau_2^2}{A_1\tau_1 + A_2\tau_2} \quad (2)$$

As a consequence, the lifetime of Ce^{3+} in Sr_3AlO_4F:1%Ce^{3+} is calculated to be 37.02 ns, then it gradually declines from 37.02 ns to 19.56 ns as the amount of Tb^{3+} ion increases in the range of 0–20%. The energy transfer efficiency (ETE) (η_T) from Ce^{3+} to Tb^{3+} can be calculated by the following formula:

$$\eta_T = 1 - \tau_{S0}/\tau_0 \quad (3)$$

where τ_S and τ_{S0} are the decay lifetime of the sensitizer (Ce^{3+}) with and without activator (Tb^{3+}) present. The maximum value for ET is found to be 51.4%.

In order to investigate the energy transfer process from Ce^{3+} to Tb^{3+} in Sr_3AlO_4F, the concentration of Ce^{3+} is fixed at an optimum doping of 0.01 with a different content of Tb^{3+}. Fig. 4 shows the emission spectra of Sr_3AlO_4F:1%Ce^{3+}, xTb^{3+} (x=0, 1%, 5%, 10%, 20%). With increasing Tb^{3+} concentration, the emission intensity for Ce^{3+} excited at 401 nm decreases monotonically. Meanwhile, the yellowish-green emission of

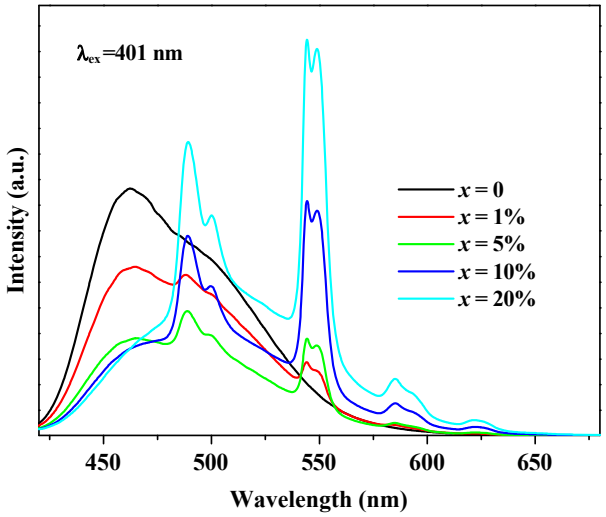

Fig. 4. The PL spectra (λ_{ex}=401 nm) of samples Sr_3AlO_4F:1%Ce^{3+}, xTb^{3+} for different Tb^{3+} concentrations: x=0, 1%, 5%, 10%, 20%.

Tb^{3+} increases gradually, which further support the occurrence of the effective energy transfer from Ce^{3+} to Tb^{3+} in Sr_3AlO_4F host.

In order to explain the energy transfer process from Ce^{3+} to Tb^{3+} in Sr_3AlO_4F, the corresponding energy levels diagrams and the possible optical transition which are involved in the energy transfer processes from Ce^{3+} to Tb^{3+} are depicted in Fig. 5. According to the measured emission wavelength of Ce^{3+} and Tb^{3+} (Fig. 2), it is probable that the energy transfer from Ce^{3+} to Tb^{3+} not that from Tb^{3+} to Ce^{3+}. When Ce^{3+} is irradiated by UV-light, electron is pumped to higher component of 5d level, and then non-radiatively relaxes to the lower component of 5d level, finally reverts to ground state by emitting two photons (457, 493 nm). Because the value of energy level of excited 5d state of Ce^{3+} is closed to the $^5D_3$ and $^5D_4$ Tb^{3+}, it is possible that energy transfer easily occurs from Ce^{3+} to Tb^{3+}, and promotes it from $^7F_6$ ground state to $^5D_3$ and $^5D_4$ of Tb^{3+}. Subsequently, the excited Tb^{3+} decays non-radiatively to the $^5D_3$ and $^5D_4$, and exhibits the intense emission of Tb^{3+} ($^5D_3 \rightarrow {}^7F_J$ and $^5D_4 \rightarrow {}^7F_J$).

According to Dexter's energy transfer formula of multipolar interaction and Reisfeld's approximation, the following relation can be obtained [29]:

$$\frac{\eta_0}{\eta} \propto C^{n/3} \tag{4}$$

where η_0 and η are the luminescence quantum efficiencies of Ce^{3+} in the absence and presence of Tb^{3+}, respectively; the values of η_0/η can be approximately calculated by the ratio of related luminescence intensity (I_{S0}/I_S); C is the concentration of Tb^{3+}; and n=6, 8, 10 correspond to dipole–dipole, dipole–quadrupole, quadrupole–quadrupole interaction, respectively. Fig. 6 gives the plots of I_{S0}/I_S–$C^{n/3}$. A liner relation can be observed when n=6, which suggests that the energy transfer from Ce^{3+} to Tb^{3+} in Sr_3AlO_4F host is dominated by the dipole–dipole mechanism.

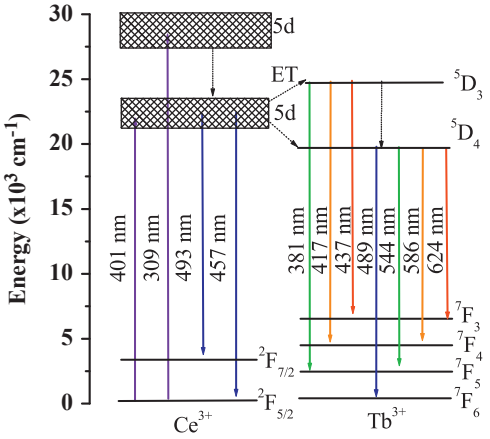

Fig. 5. Schematic energy level diagram of the ET process of $Ce^{3+} \rightarrow Tb^{3+}$ in Sr_3AlO_4F:Ce^{3+}–Tb^{3+} phosphor.

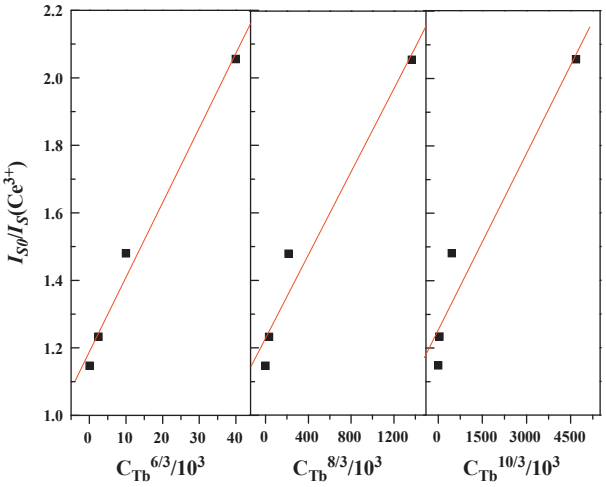

Fig. 6. Curve of I_{S0}/I_S of Tb^{3+} (a) $C_{6/3}$, (b) $C_{8/3}$, (c) $C_{10/3}$.

4. Conclusions

In conclusion, Sr_3AlO_4F:Ce^{3+}, Tb^{3+} phosphors were synthesized by the solid-state reaction under a reductive atmosphere. The spectral overlap between the emission band of Ce^{3+} and the excitation band of Tb^{3+} supports the occurrence of the energy transfer from sensitizer Ce^{3+} to activator Tb^{3+}. Ce^{3+}/Tb^{3+} co-doped Sr_3AlO_4F shows more intense yellowish-green light with emission peak at 544 nm compared to that of the Tb^{3+}-doped Sr_3AlO_4F. The energy transfer from Ce^{3+} to Tb^{3+} in Sr_3AlO_4F host has been demonstrated to be a resonant type through a dipole–dipole interaction mechanism. We can conclude that this kind in of phosphors would have potential use in the technology of white light-emitting diodes.

Acknowledgments

This work is financially supported by the National Natural Science Foundation of China (No. 20976002), the Beijing Natural Science Foundation (No. 2122012), Key Projects for

Science and Technology of Beijing Education Commission (KZ201310011013), Projects of Transformation and Industrialization of College Scientific & Technological Achievements and Projects of the Combination of Manufacture, Education & Research of Guangdong Province (No. 2011B090400100).

References

[1] P. Lauer, C.D. Rinaudo, M. Soriani, I. Margarit, D. Maione, R. Rosini, A.R. Taddei, M. Mora, R. Rappuoli, G. Grandi, J.L. Telford, Science 309 (2005) 5731.
[2] E.F. Schubert, J.K. Kim, Science 308 (2005) 1274.
[3] H.Y. Du, J.F. Sun, Z.G. Xia, J.Y. Sun, Journal of the Electrochemical Society 156 (2009) 361.
[4] M. Batentschuk, A. Osvelt, G. Schierning, A. Klier, J. Schneider, A. Winnacker, Radiation Measurements 38 (2004) 539.
[5] H. Lin, X.R. Liu, E.Y.B. Pun, Optical Materials 18 (2002) 397.
[6] Z.G. Xia, H.Y. Du, J.Y. Sun, D.M. Chen, X.F. Wang, Materials Chemistry and Physics 119 (2010) 7.
[7] T. Vogt, P.M. Woodware, B.A. Hunter, A.K. Prodjosantoso, B.J. Kennedy, Journal of Solid State Chemistry 144 (1999) 228.
[8] A.K. Prodjosantoso, B.J. Kennedy, T. Vogt, P.M. Woodward, Journal of Solid State Chemistry 172 (2003) 89.
[9] S. Park, T. Vogt, Journal of Luminescence 129 (2009) 952.
[10] Z.F. Tian, H.B. Liang, B. Han, Q. Su, Y. Tao, G.B. Zhang, Y.B. Fu, Journal of Physical Chemistry C 112 (2008) 12524.
[11] X.M. Liu, R. Pang, Z.W. Quan, J. Yang, J. Lin, Journal of the Electrochemical Society 154 (2007) 185.
[12] Z.L. Wang, H.L.W. Chan, H.L. Li, J.H. Hao, Applied Physics Letters 93 (2008) 141106.
[13] X.Y. Huang, D.C. Yu, Q.Y. Zhang, Journal of Applied Physics 106 (2009) 113521.
[14] M. Yang, H. You, K. Liu, Y. Zheng, N. Guo, H. Zhang, Inorganic Chemistry 49 (2010) 4996.
[15] V. Pankratov, A.I. Popov, S.A. Chernov, A. Zharkouskaya, C. Feldmann, Physica Status Solidi B 247 (2010) 2252.
[16] Y. Huang, K. Jang, H.S. Lee, E. Cho, J. Jeong, S.S. Yi, J.H. Jeong, J.H. Park, Physics Procedia 2 (2009) 207.
[17] H.S. Kiliaan, F.P. Herwijnen, G. Blasse, Journal of Solid State Chemistry 74 (1988) 39.
[18] H. Guo, H. Zhang, J.J. Li, F. Li, Optics Express 18 (2010) 27257.
[19] Q. Luo, X. Qiao, X. Fan, X. Zhang, Journal of Non-Crystalline Solids 356 (2010) 2875.
[20] W. Chen, H. Liang, H. Ni, P. He, Q. Su, Journal of the Electrochemical Society 157 (2010) 159.
[21] R.D. Shannon, Acta Crystallographica A 32 (1976) 751.
[22] C.H. Huang, T.W. Kuo, T.M. Chen, ACS Applied Materials and Interfaces 2 (2010) 1395.
[23] G. Blasse, B.C. Grabmaier, Luminescent Materials, Springer Verlag, Berlin, Heidelberg, 1994.
[24] G.G. Li, C. Peng, C.M. Zhang, Z.H. Xu, M.M. Shang, D.M. Yang, X.J. Kang, W.X. Wang, C.X. Li, Z.Y. Cheng, J. Lin, Inorganic Chemistry 49 (2010) 10522–10535.
[25] X.M. Han, J. Lin, J. Fu, R.B. Xing, M. Yu, Y.H. Zhou, M.L. Pang, Solid State Sciences 6 (2004) 349.
[26] G. Blasse, A. Bril, Philips Research Reports 22 (1967) 481.
[27] J. Lin, Q. Su, Journal of Materials Chemistry 5 (1995) 1151.
[28] J.Y. Sun, J.H. Zeng, Y.N. Sun, J.C. Zhu, H.Y. Du, Ceramics International 39 (2013) 1097.
[29] G. Blasse, Philips Research Reports 24 (1969) 131.